Chapter 12

Trapping and Detection of Single Molecules in Water

M. Willander, K. Risveden, B. Danielsson, and O. Nur

Summary

An innovative nanoprobe-based device that can measure and adjust the pH, can mimic biochemistry, can create microscale vortices in water, and can be used to trap single molecules is presented. Because the analytes in question to trap and detect are small in dimensions, we start by presenting scaling issues and challenging limitations for miniaturized chemical nanosensors. Advantages of using nanoprobes e.g., isolated nanowires, as the components in chemical sensing are discussed. How the observation of the physical property can beneficially change with isomorphic scaling is highlighted. Some of the technology-related constrains are presented for specific sensors. Solutions to overcome such problems are also given. Different aspects, e.g., sample size and sensitivity, for chemical sensing at the nanoscale are highlighted.

Key words: Trapping single molecules, Scaling, Miniaturized Sensors, Nanoelectronics, pH, Nanowires, Biosensors, Chemical Sensors

1. Introduction

Traditional chemical and biological analytical techniques used in various fields involve reactions that take place in solutions on addition of reagents or other bioreactive species. In addition, systems that do not involve reagents are more common and of interest. In these systems, the reagents are already immobilized. In some systems, these reactions take place at an electrode and they are commonly called *sensors (1)*. By definition, sensors are devices that are composed of an analyte-selective interface, which is connected to or in proximity to a transducer. The transduction mechanism relies on the interaction between the surface and the analyte directly or through mediators *(2)*. The analyte selective

James Weifu Lee and Robert S. Foote (eds.), *Micro and Nano Technologies in Bioanalysis*,
Methods in Molecular Biology, vol. 544
DOI 10.1007/978-1-59745-483-4_12,

interface can be a gas, a bioactive substance, a protein such as an enzyme or an antibody, a microorganism, etc. These interfaces can be very capable of recognizing, sensing, and regulating sensitivity and specificity with regard to the analyte. The transducer converts the biochemical signal into an electric signal. Finally, an amplification of the sensed signal may be needed. This implies that the sensor system is mainly composed of three subunits. Nevertheless, the sensor is sometimes referred to as the input transducer; the word transducer is derived from the Latin verb *traduco*, which means a device that transfers energy from one system to another in the same or another form. Biochemical sensors are often simple and can offer real-time analysis of human body analytes. They represent a broad area of emerging technologies ideally suited for human health care analysis. The human being's natural sensing system is a notoriously poor gauge even to approximately measure simple things like weight, length, distance, humidity, etc. Using measurement tools to help us to obtain accurate values, in general, is as old as the existence of human beings. Noah when building his ark used the cubit (the length of the arm from the tip of the middle finger to the elbow) as a standard to measure length. Today sensor science and technology require a multidisciplinary environment where biology, chemistry, physics, electronics, and technology work hand in hand to achieve the ultimate goal of a time domain, small-size, selective, and sensitive sensor. The modern sensor concept dates back to 1956, when Clark published a paper on the oxygen electrode *(3)*. Since then, sensor science and technology have evolved dramatically and become multidisciplinary. In its modern concept, which begins in 1962, a biosensor is based on the fact that enzymes can be immobilized at an electrochemical detector to form enzymatic detectors that can be used for sensing *(4)*. It is worth mentioning that bioactivity is characterized to be of a chemical nature, as will be elaborated in the next section. The main biosensor categories are divided into optical, calorimetric, piezoelectric, and electrochemical biosensors. Calorimetric or thermal biosensors, such as the enzyme thermistor developed at Lund University, have proven very versatile and scalable, and have unsurpassed operational stability *(5)*. Electrochemical biosensors respond to electron transfer, electron consumption, or electron generation during a chem/bio-interaction process. This class of sensors is of major importance and they are more flexible in terms of miniaturization (scaling down) than most other biosensors. They are further divided into conductometric, potentiometric, and amperometric devices. In conductometric sensors, the change of conductance between two metal electrodes caused by the biological reaction is measured *(6)*, whereas, in potentiometric sensors, the relative potential change is measured at a reference electrode *(7)* due to accumulation of charge (electrons)

with no current conduction. Amperometric biosensors are based on the current change caused by electron transfer in the chemical reactions at the electrodes at a certain applied voltage. The principle of operation of this class of sensors is of great importance to miniaturized future sensors.

There is an increasing need for selective, sensitive, time domain chemical sensors for physiological environments. This is driven by human health care and the need for new drug discovery. Almost all chemical and biochemical reactions involve a process where the acidity (pH) is subjected to relatively small changes, sometimes only momentarily. When considering real physiological mediums, the problem becomes more complicated because the pH changes have to be detected in volumes that are relatively quite small. This obviously implies that the new needed sensors have to also be small in dimension. In general, when objects are scaled down isomorphically (i.e., all dimensions are scaled uniformly), the change in length, area, and volume ratios increases as we scale down, and this renders surface effects to be significant. This alters the relative influence of the different physical effects in question in an unexpected way. If the object (e.g., analyte) in question shrinks to the same length scale as the boundary layer (effect), being thermal, diffusion, optical, etc., continuum theories break down and the laws of micro scaling no longer apply. This fact makes such scaled objects possess unusual properties that can be further engineered depending on the way these objects are scaled and/or arranged. Fortunately, sometimes these properties are beneficial to our nanosensors purpose, as is illustrated below. For the analyte in question, the total sample size needed for the detection is determined by the analyte concentration. The analyte concentration is in fact out of our control, i.e., sometimes we need to detect mediums with relatively very low analyte concentrations. One important property of scaled objects (sensors) of particular interest is the sensitivity of these scaled sensors. Obviously, a sensor with a wide dynamic range for detection sensitivity is indeed an aim of the scientific community. Before proceeding, we define the sensors of interest here to be those called electrochemical sensors.

In this chapter, we first present sensor domains and a brief summary of the history of using silicon in sensor technology. Because of its importance to our human health, the emphasis will be on sensors of a chemical nature because they are vital to physiological investigations. Different aspects of scaling issues and challenging limitations are briefly discussed. The nanoscale water transistor developed recently is then presented as a multifunction platform (Lab on a Chip).

1.1. Sensor Domain and Historical Background

We first need to define the different signal domains that distinguish between different types of sensors. In general, sensors are devices that make use of one or several of many different effects. Some

documented effects dates back to as early as the 18th century (thermocoupling effect). Most of the actual effects belong to six main domains *(8)*. These domains are radiant, mechanical, thermal, electrical, magnetic, and chemical.

Silicon is the dominant semiconductor material in use today, and has been explored in sensor technology both for conventional sensors as well as for state-of-the-art of nanosensors. Below, we briefly mention the history of using Si as a material for sensors. Sensors have been fabricated using many material technologies, ranging from piezoelectric quartz crystals and compound semiconductors to metals. However, the real advances in sensor technology occurred when pure germanium and, later, silicon became available. Although the availability of these two elementary semiconductors was not aimed at sensor technology, the impact cannot be neglected. An elegant review article that deals with many issues in the history of using Si in sensor technology can be found in reference *(9)*. To our knowledge, the first two Si-based sensors were based on the piezoresistive effect (the electrical to mechanical or the opposite transfer domain) and were demonstrated more than four decades ago *(10,11)*. The first was demonstrated in 1954 *(10)* and the second was published in 1970 *(11)*, although related activities started in 1965. Moreover, the emergence of silicon dioxide use and various processing techniques, especially lithography, have made Si in its pure crystalline state with controlled doping the best material choice for sensors. Nevertheless, because silicon dioxide is one of the reasons for the domination of silicon technology today, ironically silicon dioxide still plays an indirect important role in today's nanosensors. The first two pioneering chemical sensors were the ion-sensitive field effect transistor (ISFET) developed by Bergveld *(12)* and the Pd-gate metal oxide field effect transistor (MOSFET) invented by Lundström et al. *(13)*. Pd-gate MOSFET (Pd-MOSFET) operation is restricted to gaseous medium and relies on the catalytic ability of the Pd to decompose hydrogen molecules into hydrogen atoms. Nevertheless, the first "enzyme transistor" was made with a Pd-MOSFET that also showed some ammonia sensitivity *(14)*. By using hydrophobic gas-permeable membranes (e.g., Gore-Tex) as the interface between the aqueous medium and the gas phase, interesting sensor constructions could, however, be made, especially with the use of noble metals other than Pd. Sensitive ammonia detectors were made with iridium as the catalytic metal and combined with ammonia-producing enzymes to form excellent biosensors for clinically important analytes such as urea and creatinine *(15)*. On the other hand, the ISFET is suitable for operating in electrolyte medium. This has led to its usefulness for many interesting experiments for physiological investigations. This property has forced the ISFET to be the building block of the modern knowledge we have today in chemical nanosensors.

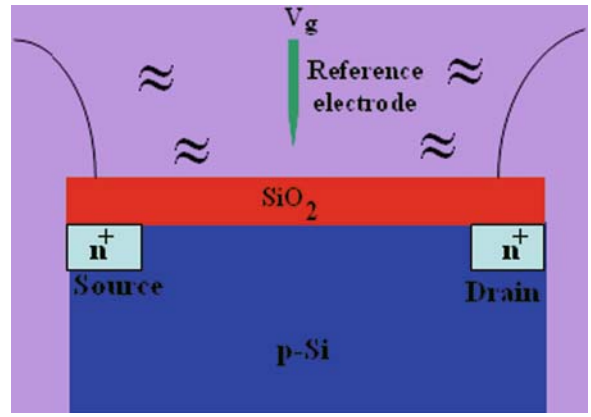

Fig. 1. Schematic diagram showing the ISFET (as an example of a conventional planar sensor) in its simplest configuration, with the metal gate replaced by a small cage to host the electrolyte.

Figure 1 shows a schematic diagram of the ISFET in its simplest form, with the gate metal replaced by a cage for hosting the electrolyte.

The need for sensors to be smaller is in fact because of two reasons, the first is the so-called nonlinear effect when using an isolated nano-electrode for sensing and the second is due to fundamental reasons (both are discussed below). To mention some examples of the state of the art of modern sensors, we choose two recently developed nanosensors, both based on Si technology. The first is the Si nanowire-based field effect transistor (SiNW-FET) *(16)*. This represents the first NANO-FET-based chemical nanosensor. It operates on a functionalized site binding approach. Using this SiNW-FET, selective sensitive time-domain sensors were demonstrated. The second example is, however, different, it is the first wet nanoscale transistor operating in the bipolar mode (presented in a separate section below) *(17)*. It relies on the control and sensitive detection of the acidity (pH) of water or any other compatible electrolyte. It can be used to mimic conditions of chemical reactions taking place in living cells as well as detecting and manipulating single molecules in a very convenient way *(18–20)*. **Figure 2** shows the outer microparts of the recently developed nanoscale wet transistor. Here the nanoscale active parts are placed within the small dark middle part in the figure. The nanoscale active parts are shown in **Fig. 3c–f**. The role of the larger parts is to adjust and control the pH.

1.2. Scaling Issues and Challenging Limitations

The ISFET has been a very interesting and useful device for sensor technology and has been a fertile tool for scientific knowledge; however, for multiple reasons, but mainly physical limitations, it is not the most suitable tool for applications that involve low concentration and single cell or molecule detection.

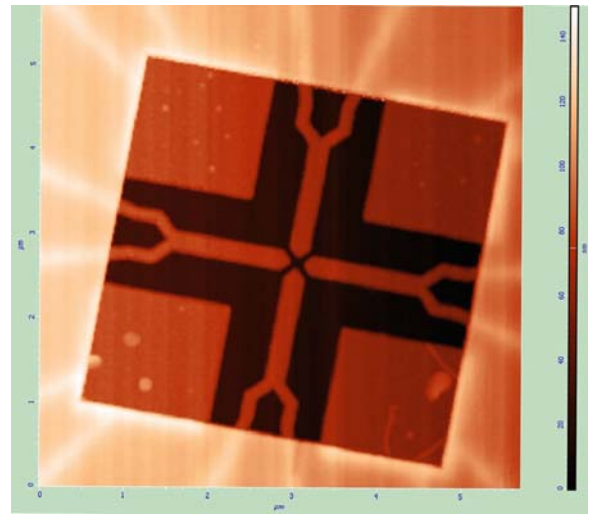

Fig. 2. Atomic force microscopy (AFM) image of the nanoscale active parts of the "wet" transistor/RISFET chip. The inner electrodes in this AFM image are separated with a 200-nm gap.

The "nonclassical" nanostructure-based sensors are more suitable for selective, sensitive, and time domain chemical sensing for many applications that involve low concentration and single cell or molecule detection.

In this section, we briefly mention some important facts and challenges regarding scaling issues, i.e., reducing the size of the sensors to smaller dimensions (specifically to the nanometer regime). Nevertheless, because of the fundamental importance of scaling issues, the present section is rather comprehensive and it discusses different aspects of scaling. When a system is reduced isomorphically in size, i.e., scaled down with all dimensions of the system decreased uniformly (isomorphic scaling), the change in length, area, and volume ratios alters the relative influence of the physical effect in question in an unexpected way *(21)*. The famous Russian nesting doll represents an illustrative example of isomorphic scaling **(Fig. 4)**. Note that the smallest doll has the largest surface area-to-volume (S/V) ratio. In other words, if the object (analyte) under focus shrinks down to the same length scale as the boundary layer (effect), being of thermal, diffusion, optical, etc., continuum theories break down and the laws of macro scaling no longer apply. When an object shrinks down, the S/V ratio is larger. This renders the surface forces and effects more important and dominating than other forces. Generally speaking, as objects decrease in size, force scaling follows the following: forces are scaled for those with a lower power of the linear dimensions in a

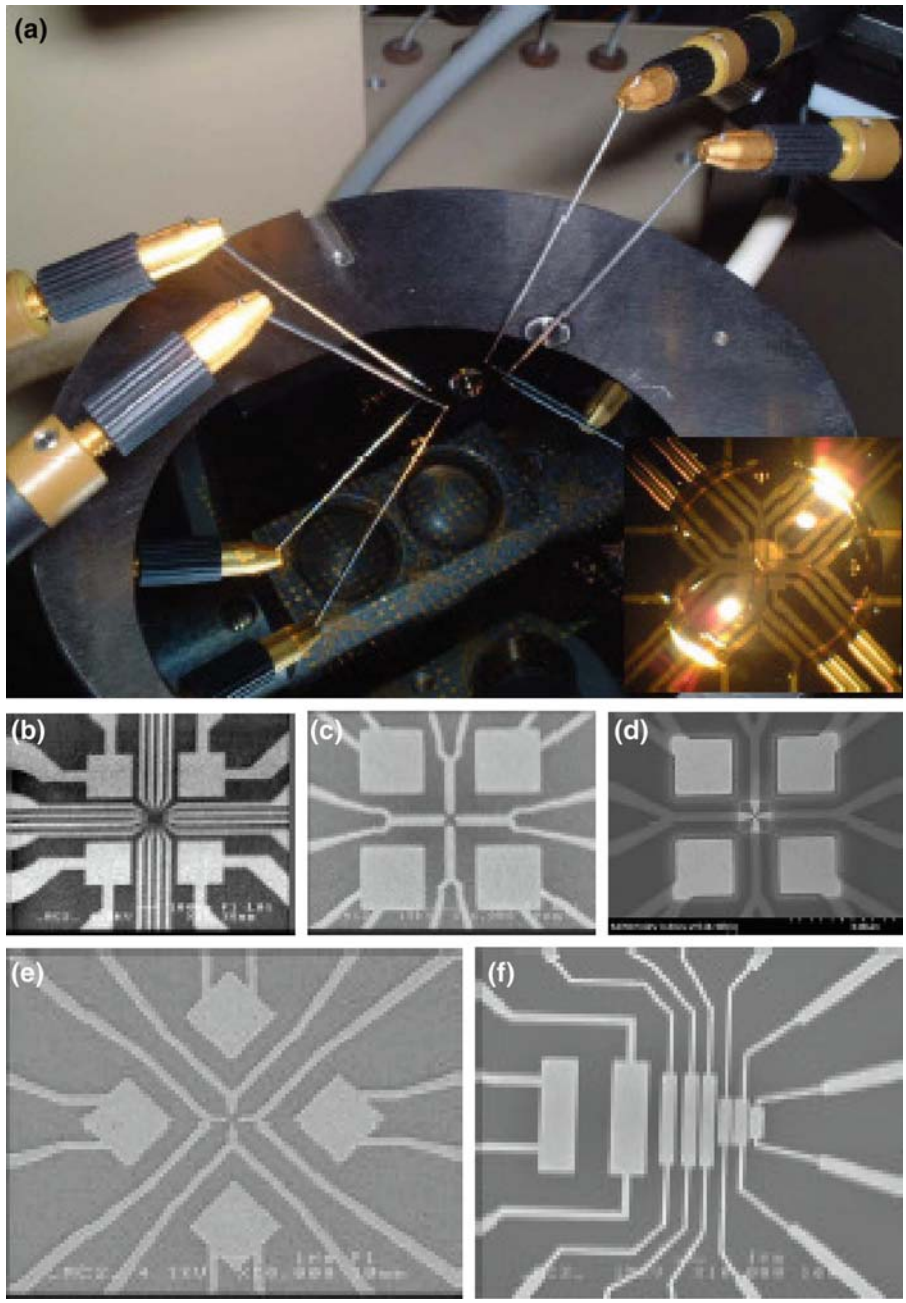

Fig. 3. (**a**) The sensor nanotransistor under measurement (the insert is a colored micrograph of the enlarged middle part showing the large pH electrodes); (**b**) scanning electron microscopy (SEM) image showing the large pH electrode (base); (**c**) SEM image of the investigated small pH electrodes; (**d**) the small pH electrode (base) and the small sensing electrodes (emitter-collector) with windows exposing the active device areas; (**e**) another design of the small electrode; and (**f**) a special design used for time-dependant electrical characterization.

Fig. 4. The famous Russian nesting dolls are an illustrative example of isomorphic scaling. The largest doll has the smallest surface to volume ratio, whereas the smallest doll has the largest ratio.

way that keeps them dominant over those with a higher power. A simple example of this is that, when considering an object with a mass m, when shrinking the dimensions, the surface tension will dominate over the gravitational force. Another example is that, for an object in an electromagnetic field, the electrostatic forces will gain over the magnetic forces if the object shrinks *(22)*. The later example has important consequences and is also one of the reasons that necessitated the need for nanosensors for detection of a small low-concentration analyte (e.g., single-molecule detection). Below we discuss the influence of the miniaturization (reduction in size) on different aspects, namely, technological challenges of nanosensors, the influence of the sample size, and the effect of the sensor size on the sensor detection sensitivity. We start by defining the sensor detection sensitivity (η) as the amount of change in the sensor's output, I_{out}, in response to a change in the sensor's input, I_{in}, over the entire sensor range (i.e., $\eta = dI_{out}/dI_{in}$). Obviously, a sensor with a wide dynamic range for the detection sensitivity is an aim of the scientific community.

1.3. Technological Challenges

In connection with technological challenges, we consider an example where liquid ejection is needed. In a real man-made sensor device, a small wet sensor must be embedded in a fluidic circuit to provide an environment for the sensor to survive (e.g., a cell). This is mentioned to emphasize why such an example is illustrative. We consider scaling down the liquid contactless ejection isomorphically, e.g., a water droplet is to be ejected, without contact, from a nozzle with different volumes. Nowadays, volumes from 10 μL down to 25 nL can routinely be ejected without contact through a commercial 8-channel dispenser assembly. Such an ejection can be made and observed, e.g., the event can be photographed. However, scaling down to smaller droplets (such as 10-nL water droplets) will lead to evaporation of the ejected droplet before observation of the

event (e.g., taking a picture of the 10-nL droplet being ejected) *(22,23)*. This simple example implies that an engineering solution for such a situation is challenging. Different approaches for such problem can be adopted, e.g., mixing the liquid with a compatible low vapor-pressure solvent (i.e., stirring). The wet environment we mentioned above (as the environment that enables the sensor to survive) can be a cell, for example, as demonstrated in **ref.** *(24)*. Here, a sophisticated experiment demonstrated that a subtle change in the concentration of ions and small molecules (≤20 nm in size) embedded inside a cell can be detected. The cell here represents the environment that kept the molecule wet. This simple example of the challenge of small (a few nanoliters of volume) aqueous matter ejection suggests that, probably, mature future chemical nanosensors will relay on engineered bacteria, proteins, etc. In addition, self-assembling to house the sensing molecules is expected to be important-ant. Self-assembling is a general term in our opinion. Conventionally, it means an engineered substrate and/or a substrate achieved by other standard processing techniques. However, we use the term self-assembling here with an insight toward non-conventional scenarios, e.g., site binding is a form of the non-conventional self-assembling scenarios intended above, but not achieved by conventional processing techniques. Naturally, this is enforced by the small size of the analyte to be sensed. Another technological appealing issue is the sensor arrays. Arraying is one way of providing fast, efficient, and consistent analysis for accurate comparative investigations. Moreover, sensor arrays with reduced signal to noise (S/N) ratio ($\approx n^{+1/2}$ for n connected identical sensors), and having enhanced selectivity/sensitivity are required. Many difficulties in achieving these requirements arise when scaling down to the sensor nanoregime. The final issue discussed before concluding this section is sensor storage and diffusive mixing. This is important and connected to the first discussed issue in this section, i.e., the aqueous wet environment challenges. Clearly, shelf-life storage of different sensor reagents is limited, and this implies that storage in a limited chemical environment should be followed by rehydration using the appropriate buffer before sensor usage. In addition, small amounts of reagents that make the sensor cocktail should be prepared according to diffusive mixing just before the sensor usage. Using this strategy increases the sensor lifetime and also opens new sensor opportunities. Hence, diffusivity is important. Considering a spherical molecule, the diffusion coefficient, D (m^2/s) is given by:

$$D = \frac{kT}{6\pi\rho r}, \tag{1}$$

where k is the Boltzmann constant (1.38×10^{-23} mJ/K), T the absolute temperature (K), ρ is the absolute viscosity (in kg/m/s), and r is the molecule hydrodynamic radius *(21)*. A molecule with molecular weight between 500 and 100 Da will have a diffusion coefficient of approximately 5×10^{-5} cm^2/s. Considering the random walk equation, the diffusion length x of a molecule in a solution is given by:

$$x = \sqrt{2Dt}\ , \tag{2}$$

where t is the time required for the molecule to diffuse over a distance x. This equation implies that the diffusion of a molecule in a bulk solution over 10 μm is a million times faster than the diffusion over 1 cm. Now considering a specific volume of a liquid (for simplicity, we take cubic volume), we consider diffusion of a molecule (contained in a fixed solution mixed with the liquid volume in question) from one side of the cube to the opposite side. We consider here the case of saline solution in a bucket *(25,26)*. Assuming a diffusion constant D of the order of 10^{-5} cm^2/s, and considering two volumes of 1 μL and 1 fL (10^{-15} L), the corresponding cube length for the molecule to diffuse across are 1 mm and 1 μm, respectively. The diffusion time t to cross a distance of 1 mm is 500 s whereas it is only 0.5 ms to diffuse across 1 μm. It is worth mentioning that in this solution reagent mixing example, the number of molecules present in the two volumes (taking a concentration of 1 μM solution) are 6×10^{11} and 600 molecules for the two solution volumes considered, respectively. From the preceding mixing example, it is evident that, although mixing is mediated by diffusion, it is fast at micro levels and this allows for reaction times dictated by inherent kinetics rather than the time it takes for the reactant species to meet in mixed solutions. This takes us back to the fact mentioned above; namely that as sensors are scaled, the physical effect in question will often be altered in an unexpected way. In nature, only the smallest species made of one or fewer cells relay purely according to diffusion, but other species made of many cells reply on other routes for transport, e.g., hearts, blood vessels, lungs, digestive system, etc. Nevertheless, from the discussion above, aqueous mixed volumes for chemical sensors should be approximately 1 mm^3 or lower if a fast sensor response is to be achieved.

1.4. Sample Size Effect

Moving from technological challenges illustrated by the above example, we proceed to the effect of the sample analyte size. Miniaturization is a mixed issue for both the sensor and the analyte. The sample volume (V) required for detecting a given analyte concentration is given by *(27)*:

$$V = \frac{1}{\phi N_A C_i}, \tag{3}$$

where is the sensor efficiency (between 1 and 0), N_A is Avogadro's number (6.02×10^{23} mol^{-1}), and C_i is the concentration of analyte i (in mol/L). This equation clearly indicates that the analyte concentration fundamentally determines the sample volume. It has been noted that numerous chemicals and other biological species are routinely present with concentrations ranging from 100 to 10^7 units-copies/mL *(25)*. Consequently, large volumes are required to sense and detect almost most of the natural analyte concentrations; e.g., a relatively large volume of approximately 100 μL is required for accurate DNA assays. If the sensor sensitivity does not scale with its size, there is no benefit in future miniaturization. Nevertheless, as we mentioned in the paragraph above, new engineered materials are needed. Fortunately, such materials are available today and they help in shifting the detection for low analyte concentration and hence reduce the sample volume size required for sensing low concentrations. Such "exotic" materials have the property of producing enhanced fluorophores. It worth mentioning that colloidal particles, as well as nanocrystals or quantum dots, also play an important role because of their ability to approximate the ideal fluorophores, i.e., nonphotobleaching, narrow emission, and symmetric with multiple resolvable color that can be excited simultaneously using a single excitation wavelength. In addition, an important property of quantum dots is that their color, for both emission and absorption, can be tuned to any color by only changing their size. This will improve and push the sensitivity to a better level. However, with our current knowledge, even the most sensitive exotic particle will only slightly improve the sensitivity, not to the level we require *(21)*. On the other hand, the extreme case of detecting "single" molecules can be achieved either by trapping, which technically means that the concentration of the molecule is infinite, or by interrogating ultrasmall (≈femtoliter) volumes, as performed in fluorescence correlation spectroscopy *(28)*. Nevertheless, some experiments demonstrated that excellent sensitivity still could be achieved by using nanoprobes. Even a single ion placed near a single electron transistor (SET) can cause observable modulation of the current. This critical issue, namely, the miniaturized sensor sensitivity, is addressed in the next section of this chapter.

1.5. Sensitivity Issues

To discuss miniaturized sensor sensitivity, we choose a special type of sensor, namely, electrochemical sensors. We have chosen electrochemical sensors because they are more flexible to miniaturization. Electrochemical sensors are divided into conductometric, potentiometric, and amperometric sensors. It is important to mention that measuring a voltage in a potentiometric sensor, such as the ISFET or ISE (ion sensitive electrode), is scaling invariant; amperometric sensors, on the other hand, measure currents and they

are affected by miniaturization. Most of the research efforts in miniaturization were focused on potentiometric sensors, although more benefit can be achieved from amperometric effect sensors, as is elaborated below and at the end of the next section.

Electrochemical reactions are governed by the electrode size with respect to the diffusion layer of the analyte to be recognized. If the diffusion layer of the analyte is of the order of the sensor electrode size, then the laws of classic macroscale electrochemistry breaks down *(21)*. This leaves us with unexpected effects; fortunately, some turn out to be beneficial to miniaturization. The total diffusion-limited current I_l on a large substrate of an area A based on diffusion-limited current i_l is given by:

$$i_1 = nFD_0 \frac{C_\infty^0}{\delta}, \tag{4}$$

where n is the number of electrons, F is the Faraday constant, D_0 is the diffusion coefficient of the reactant species, δ is the diffusion layer thickness, and C is the concentration of the bulk of the solution. This implies that the total diffusion current is $I_l = i_l Ax$, with x being the diffusion length. If we reduce the size of the sensing electrodes to sizes comparable to the thickness of the diffusion layer, and keep them isolated, nonlinear diffusion caused by curvature effects "as the electrodes are isolated" should be considered. Analysis of such a situation showed that, as the nonlinear curvature effects become more and more pronounced, more diffusion takes place, i.e., diffusion occurs from all directions and ion collection increasingly persists, leading to more ion supply to the electrode, i.e., a beneficial unexpected effect. The diffusion layer thickness δ caused by linear effects is time dependant and given by *(29)*:

$$\delta = \left(\pi D_0 t\right)^{\frac{1}{2}}, \tag{5}$$

Substituting this into the above expression for the total diffusion-limited current, namely I_l, we obtain the so-called Cottrell equation, which reads:

$$I_1 = nFAC_\infty^0 \left(\frac{C_0}{\pi t}\right)^{\frac{1}{2}}, \tag{6}$$

This equation represents the current versus time for an electrode subjected to a potential step large enough to cause surface concentration of electro-active species to reach zero. This expression is appropriate regardless of the electrode geometry or the solution stirring conditions, as long as the diffusion layer thickness is much less than the hydrodynamic boundary layer thickness.

This is applicable to stirred aqueous solutions. For unstirred (i.e., pure) solutions, the thickness of the diffusion layer is not well defined and all types of disturbances can affect the transport. Hence, to prevent random connective motion from affecting the transport to and from the electrode, we want to keep the diffusion layer thickness smaller than the hydrodynamic boundary layer thickness and we want the hydrodynamic layer thickness to be regular. Ironically, stirring "mixing" can enable us to achieve this goal, a fact that was also necessary to avoid; is other un-wanted effects, e.g. to avoid fast evaporation of small volumes of ejected aqueous, mixing for long self storage, etc. Nonlinear diffusion at the edges of a microelectrode results in deviation from the simple Cottrell equation at longer collection times. The corrected equation will then read:

$$I_1 = nFAC_{\infty}^{0}\left(\frac{C_0}{\pi t}\right)^{\frac{1}{2}} + AnFD_0\frac{D_{\infty}^{0}}{r}. \qquad (7)$$

For longer times and small electrodes, the Equation 7 predicts that the correction term can become significant (note the electrode surface area A is divided by radius of the collected species). It is also important to note that the charge transfer is located at the outer edge of the electrode. This is actually a very favorable scaling. The correction term is proportional to A/r r^1, whereas the background current I_c (associated with the Helmholtz capacitance) is proportional to r^2, thus, the ratio of the Faradic current (charging current) to the background current should decrease as the electrode radius decreases. The fact to be emphasized here is that, with single small microelectrode, the analytical current is still small enough to easily be exploited.

We have presented several advantages that could be achieved by scaling amperometric sensors. However, we conclude by the following: (1) higher mass transfer rates at ultrasmall electrodes makes it possible to experiment with shorter time scale (faster dynamics), (2) an array of closely spaced ultrasmall electrodes can lead to collection of sufficient electrogenerated species with high efficiency if designed appropriately, and (3) the preceding discussion implies that electrochemical measurement (sensing) is possible even in highly resistive media.

1.6. Size and Sensitivity

The aim of this section is to elucidate the advantages of nanostructures in chemical sensing. In addition to the previously mentioned nonlinear effects (denoted as geometrical effects), other fundamental issues are highlighted.

The key issue is due to simple thermodynamic reasons. It is difficult to detect a single bioanalyte, because the net charge of the analyte is shielded by a double layer. However, there are

two options to still get high sensitivity and be able to observe an immunological reaction. The first option is when working at low ionic conductivity. Here, we try to increase the Debye length as much as possible. In this case, we can measure the Donnan potentials. These small electrostatic surface potentials occur because of the formation of gradients of diffusible ions. The second option is when we deal with high ionic concentrations; in this case, the strong electrostatic potentials will be by far dominating the potential changes on the surface. Thus, the only way of observing an immunological reaction in this case is to make dynamic measurements. We can change the salt concentration of our solution and, for a short period of time, we can observe a transient signal caused by the rearrangement of the double layer. Why do nanowires make a difference when used as electrodes for sensing? The answer is that at low concentrations small surface potential changes become more and more visible with decreasing the nanowire dimensions (the nonlinear effects mentioned previously). The question is now the following: can we actually "observe" the net charge of our biomolecule, because the dimensions of the wire are smaller than the Debye length? There is no clear answer yet. However, from the experimental point of view, it seems that more than only the Donnan potentials or streaming potentials (electrokinetic) lead to the observed effects. If we have high salt concentrations, we end up with the same problem as for planar sensors.

2. Materials

The innovative electrochemical device used for the experiments presented here was processed using standard silicon technology. The materials used were as follows:

1. Low-doped oxidized Si 001 (resistivity 100 Ω-cm).
2. Gold was used for electrodes and electrical measurements pads.
3. PMMA electron beam resist was used for electrical isolation.

3. Methods

3.1. Device Fabrication Procedures

We used low-doped silicon as a starting substrate. A thermal high-quality oxide layer was first grown on the Si 001 wafers. The thickness of the oxide was 0.4 μm. We then combined

optical and electron beam lithography to obtain the device structure and used metal electrodes composed of gold for both the inner nanoscale electrodes and for the final out large-scale electrodes. Before deposition of the gold, a thin chromium layer (~5 nm) was deposited to enhance the adhesion of gold to the silicon dioxide at the same lift-off step. The device is composed of five different processing lithography layers. The first was composed of depositing orientation marks (global and chip marks) for the electron beam lithography and, in addition, it contained a part of the connectors of the nano-electrodes. It is important to mention that the metal connectors from the nano-electrodes to the outer measurements pads were divided into three different parts: outer (thick ~400 nm), middle (thin ~150 nm), and inner (thin ~100 nm) parts. The middle part was the one deposited during the first lithography step (optical lithography). Such division is necessary as the pads have to be thick and the inner nano-electrodes have to be very thin. This is due to the fact that the measurements pads can not be less than 0.4 μm in thickness if stable measrements are to be performed, and the small nanoelectrodes has to be thin (less than 100 nm) due to processing requirement of the fact that high resolution electron beam resist has a thickness which is not larger than the 100 nm. After that, the first electron beam lithography layer was performed to deposit the smallest electrodes, i.e., the nano-electrodes. Then this was followed by an optical lithography step to deposit the out thick electrode part containing the measurements pads. We next used electron beam resist as the insulating layer. Two electron beam steps were next; both exposed parts of the covered surface. The covering was necessary so the aqueous liquids placed on top of the electrodes could be biased from different places with no electrical shorts (*see* **Fig. 3**). The need for two different steps was because some areas were in the nanometer size (sensing electrodes), whereas others were in excess of 100 μm × 100 μm, and we are restricted by the electron beam lithography machine, which performs either at high resolution/low speed or low resolution/high speed. The large windows for pads were made in the low-resolution mode whereas the nanometer-sized window was exposed by using the high-resolution mode. More information regarding the fabrication and measurements can be found in refs. ***(17,18,20,30)*** (also *see* **Note 1**).

3.2. A Nanoprobe Tool for Trapping Single Molecules

As mentioned above, when considering sensing single molecules, trapping is the ideal approach for sensing. Technically, this means that the concentration of the molecule is infinite. Because single molecules usually exist in aqueous mediums, a flexible device is needed for such a purpose. According to the previous section, both the analyte and the detection device are to be comparable in dimensions. Because molecules have dimensions of few nanometers, a

device with these dimensions will be the ideal choice for developing a sensitive, selective platform for the trapping and detection of single molecules. Below, we introduce a recently developed nanoscale water transistor that can operate in aqueous mediums and perform multifunctions. **Figure 3** illustrates different parts of the nanoscale water transistor.

3.3. The Nanoscale Water Transistor

The basic operation of the sensor (transistor) is based on the variation of the pH of water by applying a voltage and independently measuring the current variation between the two nano-spaced electrodes. The pH control electrode plays the role of the base of the transistor, whereas the two nano-electrodes act as emitter and collector. When a voltage is applied between the emitter and base (V_{BE}), the simplest envisioned situation is that water dissociates into H_3O^+ and OH^-, consequently the pH of the water changes. In the presence of an electric field between the emitter and collector (V_{EC}), the dehydrated OH^- ions will be attracted to the collector, and a potential drop is established between the OH^- dehydrated hydroxyl ions and their images at the metal. Charge neutrality is postulated for the whole system and, therefore, OH^- dehydrated hydroxyl ions have to be compensated for by oppositely charged ions, namely the H^+ hydrated ions in the water. The hydroxyl ions are then located in a plane adjacent to the collector electrode called the inner Helmholtz plane (IHP). The hydrated ions (for simplicity, we consider H_3O^+) that diffuse from the bulk will be located at the so-called outer Helmholtz plane (OHP) *(31)*. These hydrated ions are then surrounded by water dipoles and will become nonconducting species. They cannot enter the outer layer, and, hence, a potential drop is then established between the OHP and the metal. This is the boundary condition at the metal/water electrodes emitter or collector electrodes. However, inside the bulk, the situation is different. The hydrated protons are envisioned in a number of ways. Namely, they exist as $H(H_2O)^+_n$ clusters. The most commonly existing configurations are Zundel cation ($n = 2$) and Eigen cation ($n = 4$) clusters. In the Zundel ion, the proton is placed between two water molecules, whereas, in the Eigen ion, a H_3O^+ ion is strongly bound to three water molecules. The proton kinetics in water as well as the absolute hydration free energy of H^+ ions in aqueous solutions is a topic of current research. For more information on these topics and on proton transport and kinetics in water, we refer the reader to refs. *(32–34)*. In addition, the protons have high mobility in presence of electric field and the ionic transport hops between water molecules in extended hydrogen-bonded structures (Grotthus mechanism) *(35)*. The total charge per unit area on the metal (σ) is given by the electronic charge multiplied by the difference between the number of anions and cations per

unit area *(36)*. Using the geometrical capacitance between the metal and the OHP, and proceeding, we obtain:

$$I_{EC} = (W_E / L_{EC})\sigma\mu V_{EC}, \qquad (8)$$

Here I_{EC} is the current between the emitter and collector, W_E is the emitter width, L_{EC} is the emitter to collector distance, μ is the mobility of the protonic species, and (σ) is the difference between the number of anions (dehydrated OH^-) and cations (hydrated H^+) per unit area. In deriving this expression, we only considered decomposition of water, and we have ignored other reactions that might exist *(37,38)*.

Figure 5 displays the measured *I–V* characteristics of two nano-electrodes 20-nm apart and for the choice of biasing V_{BE} between a large pH electrode **(Fig. 3b)** and a small pH electrode **(Fig. 3c)**. As observed in the figure, by applying V_{BE} with steps of 0.2 V, clear distinct I_{EC} currents with different threshold voltages were obtained. We then investigated the effect of changing the strength of the electric field, by applying V_{BE} between the two small pH electrodes shown in **Fig. 3c**. This device configuration will provide electric field strengths 1,500 times larger than the previous configuration **(Fig. 3)**.

We observed almost the same current range as shown in **Fig. 5**. The only qualitative difference was observed in the reverse direction (negative V_{EC}). For this negative V_{EC} bias, a different shift of the threshold voltage was observed compared with the previous

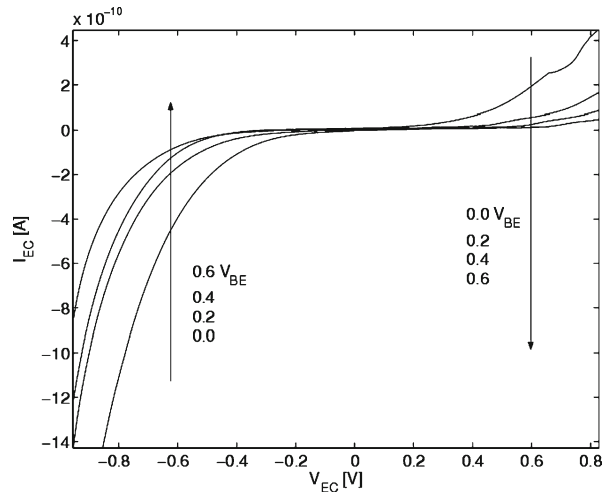

Fig. 5. The measured I_{EC}–V_{CE} of the nanoscale water-based transistor with emitter to base biasing of 0.6 V. The pH control biasing was used for a configuration that involved large pH electrodes **(Fig. 3b)** and the small pH electrodes shown in **Fig. 3c**. Reproduced from **ref.** *(17)* with permission from the American Institute of Physics.

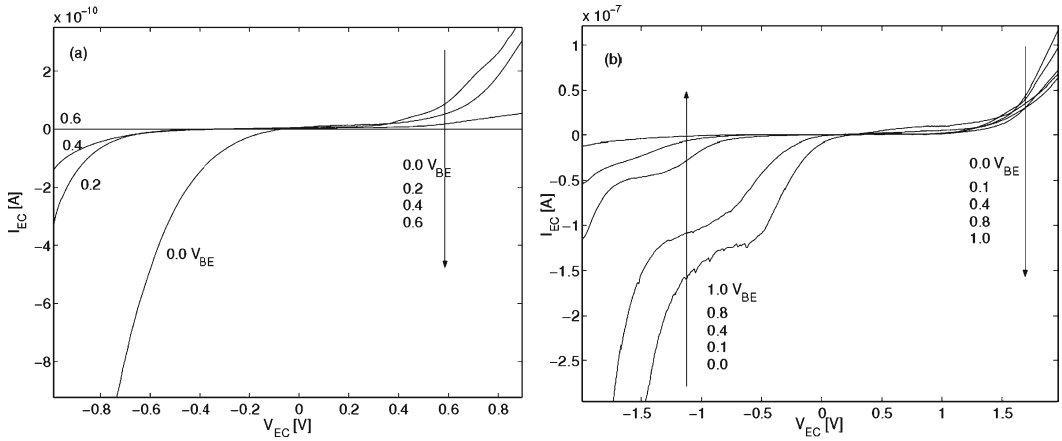

Fig. 6. *I-V* characteristics using two different designs of the small pH electrodes, (**a**) for the choice of pH electrodes shown in **Fig. 3c**, and (**b**) *I-V* obtained for the electrodes shown in **Fig. 3d**. Reproduced from **ref. (***17)* with permission from the American Institute of Physics.

behavior, as shown in **Fig. 6a**. To study the effect of the position of the pH electrode (applied electric field with regard to the applied V_{EC}), we then compared the case of **Fig. 6a** with the case using the pH electrodes of **Fig. 3e**. Here, these small pH electrodes provide the same electric field as in the case of **Fig. 6a**, but they lie along the same line joining the emitter and collector (i.e., the electric field of the pH electrodes is along the same direction as the electric field between the emitter and collector). In addition, the pH electrodes in this case are much closer to the emitter-collector nano-gap active area. The measured *I-V* characteristics are shown in **Fig. 6b**. As clearly seen, the current is now in the range of 10^{-7} A. The magnitude of the measured I_{EC} is 1,000 times larger compared with the previous two cases shown in **Figs. 5** and **6a**. Beside the observed larger current, a large shift in the threshold voltage is detected in the reverse bias direction, whereas almost no shift is observed for the forward direction (*see* **Fig. 6b**). The reason for this is attributed to the fact that, in this case, the electric field inducing the pH variation lies along the same line as the electric field between the emitter and collector that is driving the current through the device. It is also observed that, in the case of **Fig. 6b**, saturation (plateau) starts to be pronounced for negative V_{EC} and at higher positive V_{BE} values. The origin of this is a matter of present investigation. The previous DC characteristics shown in **Figs. 5** and **6a**, **b**, imply that the electric field strength for the variation of the pH (i.e., V_{BE}) alone without considering the proximity of positioning of this field has a weak influence on the output characteristics. This also indicates that the device pH sensitivity can be designed according to the application in question. The demonstrated water-based nanoscale

transistor presented here is of interest for many chemical and bioelectrical applications because of the biocompatibility of and the wide usage and presence of water in different living systems. In fact, it can be used to mimic conditions of living cells, and at the same time create microscale vortices in water *(39)*. This is in addition to the use as an efficient nanoprobe of trapping single molecules in aqueous solutions, as is demonstrated below..

3.4. Trapping Single Molecules

The ideal way of detecting single molecule is by trapping, because this implies that the molecule concentration is infinite at the trapping surface. Indeed, with the above sophisticated nanoscale water transistor, it was possible to trap and detect a single molecule *(20)*. By using a special design of the electrodes (sharp edges) of the above-mentioned nanoscale "wet" transistor and applying a radio frequency voltage between the two sharp nanoelectrodes, a strong electric field gradient is established. The use of alternating electric fields is routinely exploited for trapping biological molecules *(38)*. Depending on the temporal properties as well as the geometrical field distribution, microscopical particles (such as cells, etc.) can be moved, attracted, oriented, rotated, stretched, or trapped. This technique is supported by theories dealing with electrokinetic phenomena to help estimate the experimental conditions and confirm the observation. The technique used here is denoted as dielectrophoresis (DEP) and can lead to particle movement toward electrode edges (positive DEP) or repletion away from the electrode edge (negative DEP). Positive DEP was used and successfully trapped a single protein (R-phycoerythrin) in an aqueous solution. Using this technique, different types and sizes of molecules have been trapped in different experiments; for detailed information, we refer the reader to **ref**. *(21)* and references therein. **Figure 7a** displays the sharp electrode configuration used in the trapping experiment. In **Fig. 7b–d**, dielectrophoresis trapping of a single R-phycoerythrin protein is clearly seen because the molecule shows strong fluorescence in the cases. In **Fig. 7b**, in a protein solution of 0.6 nM and electrodes, before applying the AC voltage, no fluorescence is observed. After applying an electric field for 10 s, the molecule is trapped. In **Fig. 7d**, the scale is changed, but the experimental conditions are the same as those in **Fig. 7e**. **Figure 7e** presents results of a calculated electric field gradient. The color-coded projection shows the field gradient in the electrode plane. The upper gray enclosure defines the region where the electric field force gradient exceeds the molecular diffusion. This experiment was complemented by fluorescence correlation spectroscopy performed in the original solution (Zeiss Confocor 2). The results of this experiment indicate that up to four molecules might be present in the solution. Nevertheless, the results are shown in **Fig. 8**.

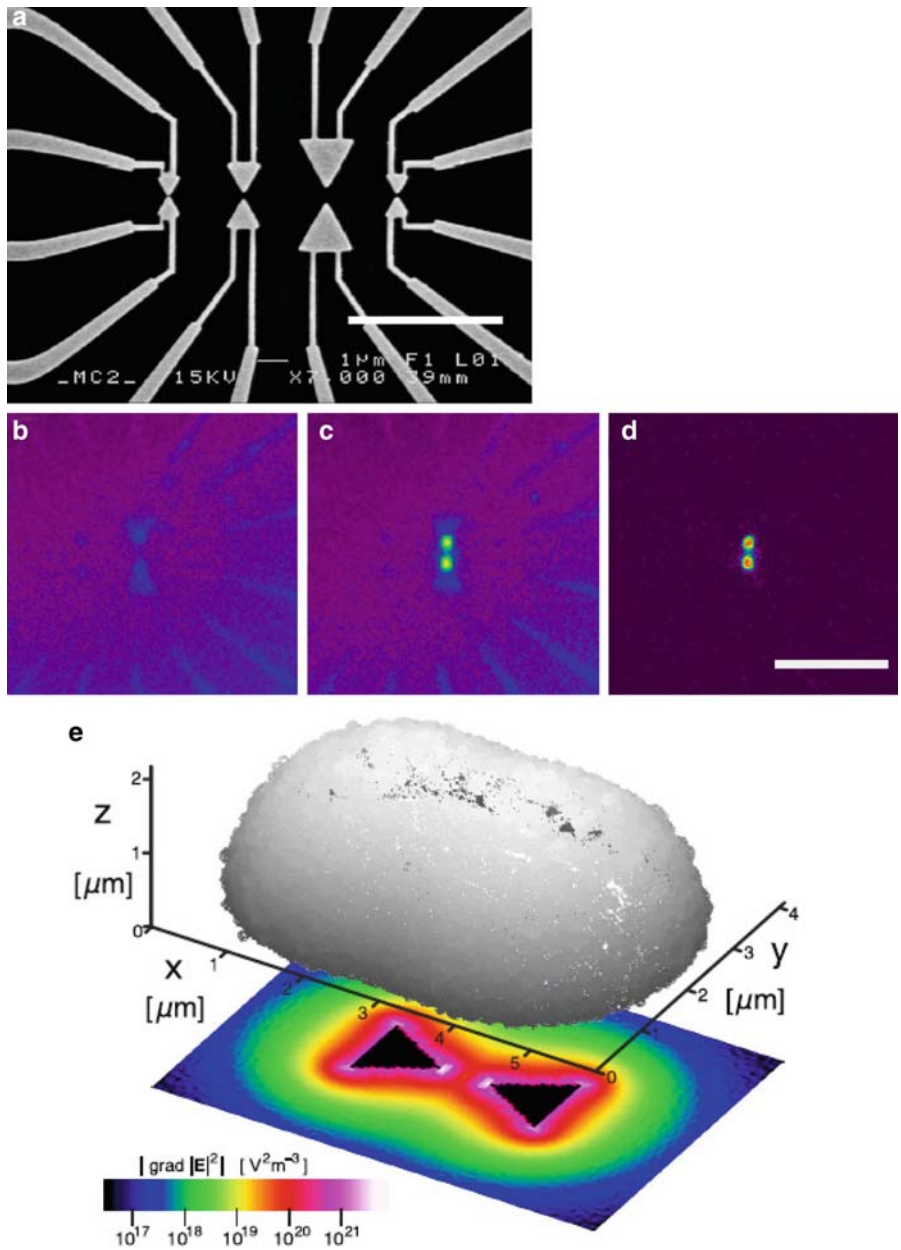

Fig. 7. (**a**) SEM showing the specially designed sharp edge electrodes, (**b**) Dielectrophoresis trapping of single R-phycoerythrin molecule between the two sharp electrodes shown in (**a**), here no field is applied and no florescence is observed. (**c**) and (**d**) field is applied and flourescence is observed. Finally in (**e**) calculated electric field gradient. Reproduced from **ref.** *(20)* with permission from the American Physical Society.

3.5. The Region Ion-Sensitive Field Effect Transistor

Recently, it was shown that the wet-transistor could be converted to a bioelectronic region ion-sensitive field effect transistor (RISFET) sensor for the detection of glucose *(30)*. In the RISFET system, the diffuse double layer above the SiO_2 surface in the vicinity of the sensing electrodes is modulated with the gate/source-drain potential. The low-profile sensing electrodes (58 ±

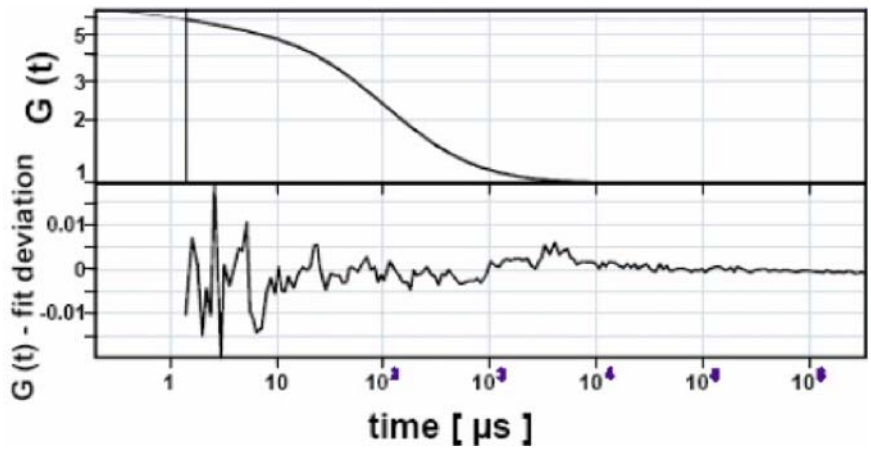

Fig. 8. Upper panel shows the florescence autocorrelation function of the R-phycoerythrin solution, and the lower panel shows the difference between the data and the numerical simulation assuming a single molecule is displayed. Reproduced from **ref.** *(20)* with permission from the American Physical Society.

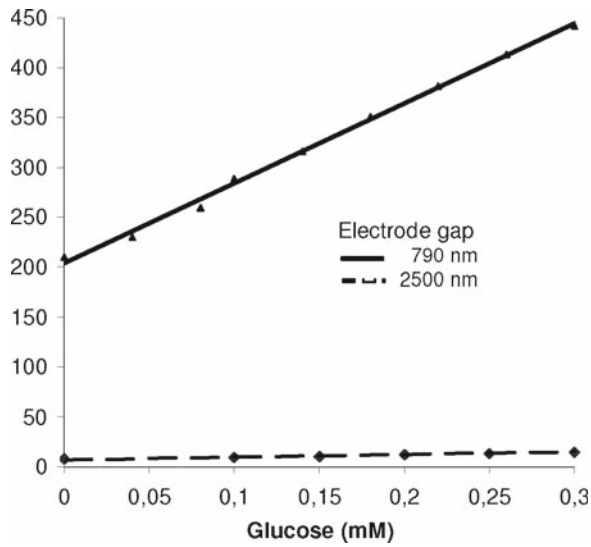

Fig. 9. The signal response current for different glucose concentrations measured with a 790-nm sensing electrode gap versus a 2,500-nm sensing electrode gap. Decreasing the size of the electrode gap enhances the sensitivity of RISFET sensor systems many fold.

2 nm high, with a median of 57.9 nm) can use this modulation to enhance the sensitivity of the sensor. Furthermore, it was shown that the field strength between the sensing electrodes had a great impact on the RISFET sensitivity. At the same applied source-drain voltage and gate potential, for two different sensing gaps, the field strength was increased approximately five times, going from a 2,500-nm gap to a 790-nm gap (*see* **Fig. 9**, x = 0–0.3 mM, y = 0–450 pA).

However, the sensitivity was increased 30 times when going from 28 to 830 pA/mM glucose. Decreasing the sensing electrode gap should enhance the sensitivity of the sensor because the field strength between the sensing electrodes would increase. Also decreasing the height of the sensing electrodes could potentially increase the sensitivity of the sensor even further, because this change would more effectively sense the modulation of the diffuse double layer. A possible way of achieving the first point is through conventional nanolithography. As for the second point, the height of the sensing electrodes could be decreased to a few hundred angstroms using conventional nanolithography, however, the introduction of conducting nanowires or nanotubes as sensing electrodes would certainly push the limits to an optimum somewhere in the vicinity of the first Helmholtz plane, as the coins are almost depleted for the favor of the desired counterions. Both suggestions are presently under investigation. The recent development of nanotrees opens up new types of nanobiosensors. **Figure 10** shows a future nanotree RISFET nanobiosensor system with gallium phosphide (GaP) nanotrees in the center of two platinum electrodes. The GaP nanotrees functions as supporting material to the catalytic enzymes of the sensor system.

3.6. Conclusion

As objects are isomorphically scaled down to the nanometer regime, some observations change in an unexpected way, sometimes this change is beneficial for the observation. Although many technological constrains appear when scaling, the advancement of nanotechnology provides possible solutions for such problems and constrains. An innovative example of a nanodevice

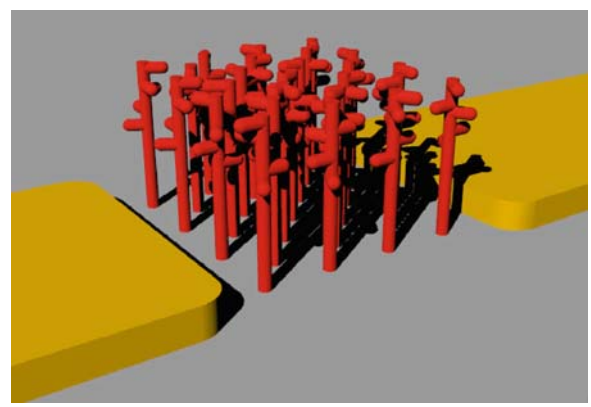

Fig. 10. A future nanotree RISFET biosensor system. Nanotrees are placed in between the sensing platinum electrodes. Enzymes are immobilized on the tops of the trunks and on the ends of the branches using thiol coupling. The substrate is measured through impedance measurements on low AC voltage in a RISFET sensor system. The impedance change of the liquid is caused by the enzymatic conversion of the substrates via the immobilized enzymes.

(multifunction platform) developed recently is highlighted as an example of achieving laboratory on a chip (lab on a chip). This nanodevice is the nanoscale water transistor, which measures and adjusts the pH value, can mimic biochemistry, can create microscale vortices in aqueous mediums, and can trap single molecules. Owing to the critical need of human health monitoring, much research is still needed to provide mature, reliable nanosensors.

4. Notes

1. The difficulty in fabricating such a device can arise from the fact that high- and low-resolution modes in electron beam lithography are combined. The metal contact from the measurement pads to the nanosensing electrode is composed of three different parts, each requiring a separate lithography step, two steps using low-resolution lithography and the final step using high-resolution lithography. In the low-resolution starting step, a thick metal layer, usually approximately 400 nm, is deposited and followed by a metal lift-off technique. The final high-resolution step is associated with thin metal lift-off and breakage at corners can lead to a nonworking device. To avoid this problem, the fabrication process is started by the middle metal layer lithography (low resolution) and a rather thin metal layer is deposited followed by lift-off. This is the middle layer. Together with this layer, alignment marks are deposited. This is followed by the other low-resolution lithography step, to form the metal line leading to the measurement pads. Here a thick metal is deposited. Finally, the high-resolution step is performed and a thin metal is deposited after lithography. In this way, metal breakage at corners is avoided and a reliable device consisting of nanoparts as well as microparts is achieved.

References

1. Wilson, G. S., Hu, Y. (2002). Enzyme based nano-sensors for in-vivo measurement. *Chem. Rev.* **100**, 2693–2704
2. Patolsky, F., Lieber, C. M. (2005). Nanowires nanosensors. *Materials Today* **8**, 20–28
3. Clark, Jr., L. C. (1956). Monitor and control of blood and tissue oxygen tensions. *Trans. Am. Artif. Inter. Organs* **2**, 41–57
4. Lyons, C., Clark, Jr., L. C. (1962). Electrode systems for continuous monitoring in cardiovascular surgery. *Ann. N. Y. Acad. Sci.* **102**, 29–45
5. Xie, B., Danielsson, B. (2007). Thermal biosensor and microbiosensor techniques. In: Handbook of Biosensors and Biochips (C. Lowe, et al. eds.). John Wiley & Sons, New York
6. Archer, M., Christopherson, M., Fauchet, P. M. (2004). Microporous silicon electrical sensor for DNA hybridization detection. *Biomed. Microdevices* **6**, 203–211

7. Koncki, R., Lenarczuk, T., Radomska, R., Glab, S. (2001). Optical biosensors based on Prussian blue films. *Analyst* **126**, 1080–1085
8. Middelhoek, S., Noorlag, D. J. (1982). Signal conversion in solid state transducers. *Sens. Actuators* **2**, 211–228
9. Middelhoek, S. (2000). Celebration of the tenth transducers conference: the past, present and future of transducer research and development. *Sens. Actuators A* **82**, 2–23
10. Smith, C. S. (1954). Piezoresistance effect in germanium and silicon. *Phys. Rev.* **94**, 42–49
11. Wise, K. D., Angle, P. D. (1970). An integrated-circuit approach to extra cellular microelectrodes. *IEEE Trans. Biomed. Eng.* **17**, 238–247
12. Bergveld, P. (1970). Development of an ion-sensitive solid-state device for neurophysiological measurements. *IEEE Trans. Biomed. Eng.* **17**, 70–71
13. Lundström, I., Shivaraman, M. S., Svensson, C. M. (1975). Hydrogen sensitive MOS structures. *J. Appl. Phys.* **46**, 3876–3881
14. Danielsson, B., Lundström, I., Mosbach, K., Stiblert, L. (1979). On new enzyme transducer; the enzyme transistor. *Anal. Lett.* **12**, 1189–1199
15. Winquist, F., Lundström, I., Danielsson, B. (1986). Determination of the creatinine by an ammonia sensitive semiconductor structure and immobilized enzymes. *Anal. Chem.* **58**, 145–148
16. Cui Y., Yei, Q., Lieber, C. M. (2001). Functional nanoscale electronic devices assembled using silicon nanowire building blocks. *Science* **291**, 851–853
17. Chiragwandi, Z., Nur, O., Willander, M., Calander, N. (2003). DC characteristics of a nanoscale water based transistor. *Appl. Phys. Lett.* **83**, 5310–5312
18. Chiragwandi, Z., Nur, O., Willander, M., Panas, I. (2005). Vortex rings in pure water under static external electric field. *Appl. Phys. Lett.* **87**, 153109–3
19. http://physicsweb.org/articles/news/9/10/7
20. Hözel, R., Calander, N., Chiragwandi, Z., Willander, M., Bier, F. (2005). Trapping single molecules by dielectrophoresis. *Phys. Rev. Lett.* **95**, 128102–4
21. Madou, M. J., Cubiccoiotti, R. (2003). Scaling issues in chemical and biological sensors. *Proc IEEE.* **91**, 830–38
22. Madou, M. J. (2002). Fundamentals of Microfabrication, 2nd edition. CRC, Boca Raton, FL
23. http://www.seyonic.com/flow.htm
24. Kopelman, R., Miller, M. T., Brause, M., Clark, H. A. (1999). Optochemical nanosensors for intracellular chemical measurement. *Proc. SPIE (Int. Soc. Opt. Eng.)* **3540**, 198–205
25. Harrision, D. J., Seilier, K., Manz, A., Fan, Z. (1992). Chemical analysis and electrophoresis systems integrated on glass and silicon chip. In: Technical Digest IEEE Solid State Sensors and Actuators Workshop, pp. 110–118
26. Brown, P. R., Grushka, E. (1993). Advances in Chromatography. Marcel Dekker, New York, pp. 50–51
27. Petersen, K., McMillan, W., Kovacs, G., Northrup, A., Christel, L. (1998). Toward next generation clinical diagnostic instruments: scaling and new processing paradigms. *Biomed. Microdevices* **1**, 43–49
28. Eigen, M., Rigler, R. (1994). Sorting single molecuels: application to diagnostics and evolutionary biotechnology. *Proc. Natl. Acad. Sci. U.S.A.* **91**, 5740–5747
29. Bausells, J., Carrabina, J., Errachid, A., Merlos, A. (1999). A simple REFET for pH detection in differential mode. *Sens. Actuators* **B57**, 56–62
30. Risveden, K., Pontén, J. F., Calander, N., Willander, M., Danielsson, B. (2007). The region ion sensitive field effect transistor, a novel bioelectronic nanosensor. *Biosens. Bioelectron.* **22**, 3105–3112
31. Mott, N. F., Twose, W. D. (1961). The theory of impurity conduction. *Adv. Phys.* **10**, 107–163
32. Walbran, S., Kornyshev, A. A., (2001). Proton transport in polarizable water. *J. Chem. Phys.* **114**, 10039–10048
33. Grabowski, P., Riccardio, D., Gomez, M. A., Asthagiri, D., Pratt, L. R. (2002). Quasichemical theory and the standard free energy of H+(aq). *J. Phys. Chem.* **106**, 9145–9148
34. Kornyshev, A. A., Kuznetov, A. M., Spohr, E., Ulstrup, J. (2003). Kinetics of proton transport in water. *J. Phys. Chem. B* **107**, 3351–3366
35. Pectina, O., Schmickler, W. (1998). A model for electrochemical proton transfer reactions. *Chem. Phys.* **228**, 265–277
36. Atkins, P., de Paula, J. (2002). Atkin's Physical Chemistry, 7th edition. Oxford University Press, New York,271
37. Kek, D., Bonanos, N., Mogensen, M., Pejovink, S. (2000). Effect of electrode material on the oxidation of H2 at the metal-Sr0.995Ce0.95Y0.05O2.970 interface. *Solid State Ionics* **131**, 249–259
38. Pohl, H. A. (1987). In: Dielectrophoresis. Cambridge University Press, Cambridge, England
39. http://spie.org/x8832.xml